

Effect of Lattice Anions on the Ligand Substitution Reaction of Tris-(1,10-phenanthroline)metal(II) Complexes: $[M(\text{phen})_3]\text{SO}_4$ and $[M(\text{phen})_3]\text{X}_2$ (M: Fe(II), Co(II), Ni(II); X: Cl^- , Br^- , I^-)

Shoji YAMASAKI, Terufumi FUJIWARA,* and Yuroku YAMAMOTO†
Department of Chemistry, Faculty of Science, Hiroshima University,
Higashisenda, Naka-ku, Hiroshima 730

†Environmental and Safety Engineering Department, Fukui Institute of Technology,
Gakuen, Fukui 910
(Received January 28, 1987)

The kinetics of the ligand substitution reaction of the title complexes in the solid state have been studied using thermogravimetry (TG) and differential scanning calorimeter (DSC) techniques. For these complex salts, an exothermic peak appears in the DSC curve which correlates with a ligand substitution in which anionatobis(1,10-phenanthroline)metal(II) complexes are formed. The heats of the exothermic reaction for ligand substitution of the sulfates decrease in the order $\text{Co(II)} > \text{Ni(II)} > \text{Fe(II)}$. Isothermal and nonisothermal kinetic analyses were carried out using the exothermic peak. Activation energies of the ligand substitution for the same counterion generally increase with the metal in the order $\text{Co(II)} < \text{Ni(II)} < \text{Fe(II)}$ and for the same metal, Ni(II) or Fe(II), increase with the counterion in the order $\text{Cl}^- < \text{Br}^- < \text{I}^- < \text{SO}_4^{2-}$. However, for the cobalt complex, the activation energies are almost identical for this series of counterions. From the trends in activation parameters for the ligand substitution, we propose a dissociative mechanism for the sulfates of all complexes studied and for the cobalt complex halides studied. For the halides of the iron(II) and nickel(II) complexes studied, a mechanism involving nucleophilic attack of the halide ions is important.

The ligand substitution reaction and the solvent exchange reaction of complex compounds in solution media have been studied by many workers.¹⁾ However, only a few studies concerning such reactions in the solid phase have been done. One reason for this lack of effect is because it is difficult to estimate contributions from the lattice anions.

Counterions play an important role in reactions such as catalysis, due to their donicity. For example, the racemization of $[\text{Ni}(\text{phen})_3]^{2+}$ is accelerated by the pairing of the complex ion with a counterion in water-*t*-BuOH. The rate increases in the order²⁾ $\text{ClO}_4^- < \text{I}^- < \text{Br}^- < \text{Cl}^-$. Moreover, we showed that since lattice anions in the solid state are in contact with the complex ion, the mechanism of the racemization could be determined by studying the effect of the donicity of lattice anions on the kinetic parameters.³⁾ We reported that such lattice anions affect the ligand substitution reaction in the solid state⁴⁾ as well as the racemization.

In this paper, the mechanism of the ligand substitution reaction of tris(1,10-phenanthroline) iron(II), nickel(II), and cobalt(II) salts (chloride, bromide, iodide, and sulfate) is investigated from the point of view of the effect of lattice anions on the kinetic parameters. By comparing kinetic information on the racemization mentioned above with that of ligand substitution, it was found that two types of mechanisms operate, depending on the donicity of the counterion, and M-N bond strengths.

Experimental

Materials. The complex salts, $[M(\text{phen})_3]\text{X}_2 \cdot n\text{H}_2\text{O}$ (M: Fe(II), Co(II), Ni(II); X: Cl^- , Br^- , I^- ; $n=7$ for chloride, 6 for

bromide, and 2 for iodide) and $[M(\text{phen})_3]\text{SO}_4 \cdot 10\text{H}_2\text{O}$, were prepared by the usual procedures.⁴⁾ The crude products were recrystallized three times from water, and dried in air. All the complexes were powdered by grinding with an agate mortar and pestle (200—270 mesh). Found: C, 53.26; H, 4.13; N, 10.36%. Calcd for $\text{C}_{36}\text{H}_{38}\text{O}_7\text{N}_6\text{Cl}_2\text{Fe}$: C, 54.49; H, 4.83; N, 10.59%. Found: C, 54.15; H, 4.50; N, 10.34%. Calcd for $\text{C}_{36}\text{H}_{38}\text{O}_7\text{N}_6\text{Cl}_2\text{Co}$: C, 54.28; H, 4.81; N, 10.55%. Found: C, 54.51; H, 4.25; N, 10.37%. Calcd for $\text{C}_{36}\text{H}_{38}\text{O}_7\text{N}_6\text{Cl}_2\text{Ni}$: C, 54.30; H, 4.81; N, 10.55%. Found: C, 52.13; H, 3.71; N, 10.01%. Calcd for $\text{C}_{36}\text{H}_{36}\text{O}_6\text{N}_6\text{Br}_2\text{Fe}$: C, 50.02; H, 4.20; N, 9.72%. Found: C, 48.74; H, 3.69; N, 9.74%. Calcd for $\text{C}_{36}\text{H}_{36}\text{O}_6\text{N}_6\text{Br}_2\text{Co}$: C, 49.85; H, 4.18; N, 9.69%. Found: C, 50.16; H, 3.64; N, 9.58%. Calcd for $\text{C}_{36}\text{H}_{36}\text{O}_6\text{N}_6\text{Br}_2\text{Ni}$: C, 49.86; H, 4.18; N, 9.69%. Found: C, 48.80; H, 3.10; N, 9.39%. Calcd for $\text{C}_{36}\text{H}_{28}\text{O}_2\text{N}_6\text{I}_2\text{Fe}$: C, 48.79; H, 3.18; N, 9.48%. Found: C, 48.69; H, 2.91; N, 9.54%. Calcd for $\text{C}_{36}\text{H}_{28}\text{O}_2\text{N}_6\text{I}_2\text{Co}$: C, 48.62; H, 3.17; N, 9.45%. Found: C, 51.38; H, 3.34; N, 10.21%. Calcd for $\text{C}_{36}\text{H}_{28}\text{O}_2\text{N}_6\text{I}_2\text{Ni}$: C, 48.63; H, 3.17; N, 9.45%. Found: C, 49.70; H, 4.26; N, 9.49%. Calcd for $\text{C}_{36}\text{H}_{44}\text{O}_{14}\text{N}_6\text{SFe}$: C, 49.55; H, 5.08; N, 9.63%. Found: C, 49.94; H, 4.50; N, 9.67%. Calcd for $\text{C}_{36}\text{H}_{44}\text{O}_{14}\text{N}_6\text{SCo}$: C, 49.37; H, 5.06; N, 9.60%. Found: C, 47.64; H, 5.86; N, 9.20%. Calcd for $\text{C}_{36}\text{H}_{44}\text{O}_{14}\text{N}_6\text{SNi}$: C, 49.36; H, 5.07; N, 9.60%.

Kinetic Methods. Under linear heating conditions, the Reich-Stivala method⁵⁾ and the direct Arrhenius method were used. The Reich-Stivala method is based on the well-known expression involving mechanisms for homogeneous kinetics, i.e.

$$\ln [g(\alpha)T^{-2}] = -E_a R^{-1} T^{-1} + \ln [ARP(RH)^{-1} E_a^{-1}] \quad (1)$$

where, $P=1-2X+6X^2-24X^3+120X^4-\dots$; $X=RT/E_a$; $(RH)=$ heating rate; α =fractional conversion; the symbols, T , R , A , E_a , have their usual meanings.⁶⁾ The following equation can readily be obtained from Eq. 1.

$$U(1) \ln [g(\alpha_1)g(\alpha_2)^{-1}T(1)] = E_a/R, \quad (2)$$

where $T(1)=(T_2/T_1)^2$; $U(1)=T_1T_2/(T_1-T_2)$. Data were fitted to Eq. 2 by iterative calculations and the most probable function $g(\alpha)$ can be obtained when the minimum standard deviation of E_a/R is attained. The reaction rate $d\alpha/dt$ is given directly from differential scanning calorimeter (DSC) and thermogravimetric (TG) experiments.

Under isothermal conditions, the Arrhenius method was used. In this study, the conversion coefficient α corresponding to the concentration of the reactant in the liquid or gas phase, can be derived from the ratio of the area corresponding to heat evolved up to a certain heating time (t_1) to the integral area of the total reaction heat obtained by DSC (Fig. 1), or the mass lost up to a time (t_1), divided by the total mass loss, determined by TG analysis. More than 5 runs for each system were carried out, and the average and the standard deviation were calculated.

Measurements. DSC and TG measurements were performed using a Sinku-Riko Model ULBAC DSC-1500L and Sinku-Riko Model TGD-3000RHN instruments, respectively. The DSC instrument was calibrated⁶⁾ from the heat of fusion of indium (99.999%), mp 156 °C, $\Delta H(\text{fusion})=3.26$ kJ mol⁻¹. Dry nitrogen flowed through the system. The finely ground samples (200–270 mesh) were placed in an aluminium cell for the DSC measurement. The sample mass was varied until a linear relationship between mass and peak area or height was obtained. Table 1 presents the

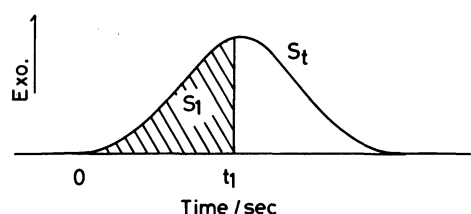


Fig. 1. Determination of reaction kinetics based on a part of the DSC curves. S_t : total area of this peak; S_1 : the area evolved up to the heating time t_1 . Conversion coefficient $\alpha_1=S_1/S_t$.

average activation energy obtained by more than 5 runs of the ligand substitution reaction at various heating rates. No significant change of the activation energy with different heating rates was appeared. In this study, a heating rate of less than 6 K min⁻¹ was used throughout the experiment unless otherwise stated. Infrared spectra were obtained by the nujol method with a JASCO Model A-102 Infrared spectrometer.

Results

Typical TG and DSC curves for $[M(\text{phen})_3]\text{SO}_4 \cdot 10\text{H}_2\text{O}$ [$M=\text{Fe}(\text{II}), \text{Co}(\text{II}), \text{Ni}(\text{II})$] are shown in Fig. 2. An exothermic peak is observed on the DSC curves and the TG curve shows that there is no loss of mass during this process. This is similar to the results already reported for the bromides of the iron and nickel complexes.⁴⁾ The heat of this exothermic reaction ($-\Delta H$) was determined from the area of the peak. The results obtained for the sulfates and the halides are given in Table 2, with the temperatures

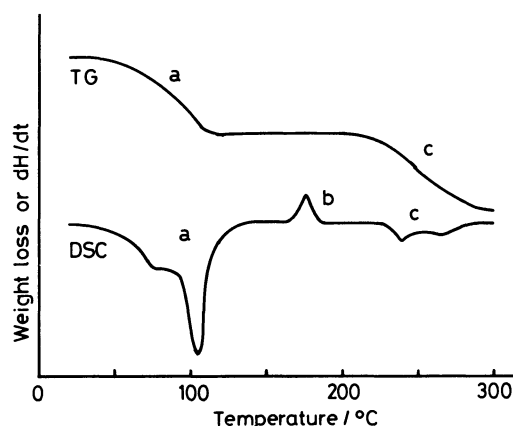


Fig. 2. Typical TG and DSC curves for $[\text{Co}(\text{phen})_3]\text{SO}_4 \cdot 10\text{H}_2\text{O}$. Heating rate is 6 K min⁻¹. a: Vaporization of H_2O ; b: exothermic peak with ligand substitution; c: vaporization of 1,10-phenanthroline.

Table 1. Effect of Heating Rate on Activation Energy of 1,10-Phenanthroline Substitution of Tris(1,10-phenanthroline)nickel(II) Sulfate Decahydrate

Heating rate/K min ⁻¹	10	8	6	4	2
$E_a/\text{kJ mol}^{-1}$	236 ± 60	201 ± 21	227 ± 28	235 ± 12	200 ± 52

Table 2. The Heat of Reaction, $-\Delta H$ of 1,10-Phenanthroline Substitution and the Peak Temperature, T_p ,^{a)} for $[M(\text{phen})_3]\text{SO}_4$ and $[M(\text{phen})_3]\text{X}_2$

Counterion	Fe(II)		Ni(II)		Co(II)	
	$-\Delta H/\text{kJ mol}^{-1}$	$T_p/^\circ\text{C}$	$-\Delta H/\text{kJ mol}^{-1}$	$T_p/^\circ\text{C}$	$-\Delta H/\text{kJ mol}^{-1}$	$T_p/^\circ\text{C}$
SO_4^{2-}	13.9 ± 1.1	175	31.9 ± 1.5	183	51.9 ± 4.2	179
Cl^-	10.8 ± 0.9	155	6.3 ± 0.2	194	13.5 ± 0.7	139
Br^-	12.7 ± 0.9	194	24.7 ± 2.7	234	7.7 ± 0.5	187
I^-	—	—	—	—	4.5 ± 0.5	170

a) T_p : The temperature at which the exothermal peak appears on the DSC curves.

(T_p) at which the exothermic peak appears. The $-\Delta H$ values for the sulfates decrease with the metal in the order $\text{Co(II)} > \text{Ni(II)} > \text{Fe(II)}$, although the peak temperatures are almost equal for this series of metals. The amount of heat evolved at any time divided by the total heat corresponds to the degree of progress of the phen substitution for the complex salts except for the iodides of the iron and nickel complexes. The iodides undergo phen substitution at a temperature higher than 220°C , which is the boiling point of 1,10-phenanthroline. 1,10-Phenanthroline molecules therefore evaporate rapidly out of the system as soon as they are released from the complexes.⁴⁾ The result is that the mass loss is related to the degree of progress of the phen substitution.

The sulfatobis(1,10-phenanthroline)metal(II) complexes, $[\text{M}(\text{phen})_2\text{SO}_4] \cdot n\text{H}_2\text{O}$ [$\text{M}=\text{Fe(II)}$, $n=1$; $\text{M}=\text{Co(II)}$, $n=0$; $\text{M}=\text{Ni(II)}$, $n=0$], were obtained as products of the ligand substitution by using the TG techniques for the sulfates. Found: C, 54.36; H, 3.07; N, 10.66%. Calcd for $\text{C}_{24}\text{H}_{18}\text{O}_5\text{N}_4\text{SFe}$: C, 54.36; H, 3.42; N, 10.56%. Found: C, 55.29; H, 3.14; N, 10.85%. Calcd for $\text{C}_{24}\text{H}_{16}\text{O}_4\text{N}_4\text{SCo}$: C, 55.93; H, 3.13; N, 10.87%. Found: C, 55.73; H, 3.15; N, 10.78%. Calcd for $\text{C}_{24}\text{H}_{16}\text{O}_4\text{N}_4\text{SNi}$: C, 55.95; H, 3.13; N, 10.88%.

The Freeman-Carroll,⁷⁾ Coats-Redfern,⁸⁾ and Reich-Stivala⁹⁾ methods were applied to the data obtained from the ligand substitution observed here. Preliminary experiments showed that the Freeman-Carroll method involving the n order reaction gave unfavorable fits to the data curves. Analysis by the Coats-Redfern method or the Reich-Stivala method involving the function $g(\alpha)$ depending on processes controlling the reaction rates of solids, gave the best fits, using computer simulations. In this study, we employed the Reich-Stivala method as described

above, due to its greater convenience. Avrami-Erofeyev functions based on the different nucleation and growth mechanisms⁹⁾ were selected to give the best possible fits of the substitution kinetic data for most of the complex salts, under linear heating conditions. However, the best fitting function could not be obtained only by the linear heating method because of a lack of significant differences in the relative errors obtained using the different functions (Table 3). Therefore the isothermal method was also applied and the best fitting function of a group of Avrami-Erofeyev functions was found. Figure 3 shows the degree of fitting for each function. A straight line is

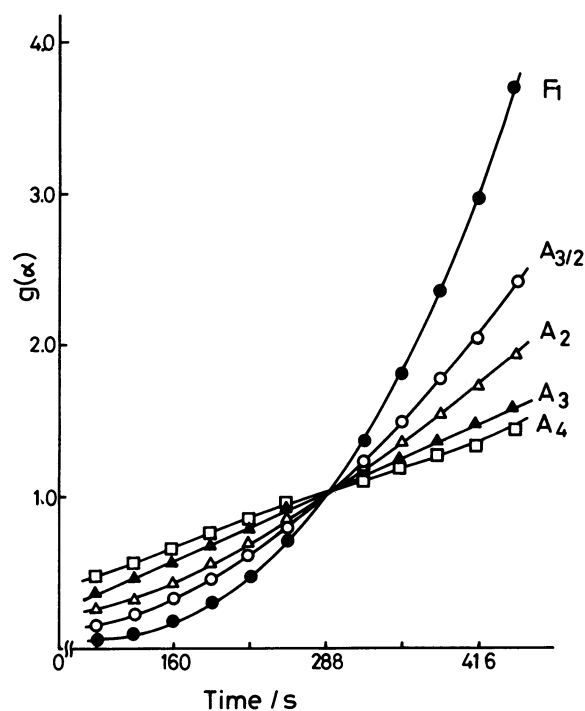


Fig. 3. Kinetic analysis for $[\text{Co}(\text{phen})_3]\text{SO}_4 \cdot 10\text{H}_2\text{O}$ under isothermal conditions at 150°C . Notation of Sharp and co-workers (Ref. 10) is used.

Table 3. Estimation of Activation Energy Using the Reich-Stivala Method for Tris(1,10-phenanthroline)-cobalt(II) Sulfate Decahydrate

Function		$E_a/\text{kJ mol}^{-1}$	% Error
Notation ^{a)}	$g(\alpha)$		
F_1	$-\ln(1-\alpha)$	334.4 ± 8.19	2.45
$A_{3/2}$	$[-\ln(1-\alpha)]^{2/3}$	220.5 ± 5.45	2.47
A_2	$[-\ln(1-\alpha)]^{1/2}$	163.6 ± 4.09	2.50
A_3	$[-\ln(1-\alpha)]^{1/3}$	106.6 ± 2.72	2.55
A_4	$[-\ln(1-\alpha)]^{1/4}$	78.1 ± 2.03	2.60
R_1	α	236.4 ± 18.96	8.02
R_2	$1 - (1-\alpha)^{1/2}$	278.1 ± 10.74	3.86
R_3	$1 - (1-\alpha)^{1/3}$	295.1 ± 7.45	2.52
D_1	α^2	480.1 ± 37.90	7.89
D_2	$(1-\alpha)\ln(1-\alpha) + \alpha$	582.4 ± 29.43	5.57
D_3	$[1 - (1-\alpha)^{1/3}]^2$	597.5 ± 14.88	2.49
D_4	$(1-2\alpha/3) - (1-\alpha)^{2/3}$	550.7 ± 24.46	4.44

a) Notation of Sharp and co-workers (Ref. 10) is used.

Table 4. Comparison of Activation Parameters Calculated by the Reich-Stivala and Arrhenius Methods^{a)} for 1,10-Phenanthroline Substitution of $[\text{M}(\text{phen})_3]\text{SO}_4$

Metal		Reich-Stivala method	Arrhenius method
Fe(II)	$\Delta H^*/\text{kJ mol}^{-1}$	361 ± 32	$350 \pm 0.8^b)$
	$E_a/\text{kJ mol}^{-1}$	368 ± 32	$352 \pm 0.8^b)$
Ni(II)	$\Delta H^*/\text{kJ mol}^{-1}$	219 ± 28	$254 \pm 0.7^b)$
	$E_a/\text{kJ mol}^{-1}$	227 ± 28	$262 \pm 0.7^b)$
Co(II)	$\Delta H^*/\text{kJ mol}^{-1}$	94 ± 7	$97 \pm 3.3^c)$
	$E_a/\text{kJ mol}^{-1}$	102 ± 7	$105 \pm 3.3^c)$

a) The best fitting function, A_3 , for the sulfates (Table 5) is used. b) Isothermal conditions. c) Linear heating conditions.

Table 5. The Best Fitting Function^{a)} and Kinetic Parameters for 1,10-Phenanthroline Substitution of the Sulfates and Halides of Tris(1,10-phenanthroline)metal(II) Complexes in the Solid State

Metal		Counterion			
		Cl ⁻	Br ⁻	I ⁻	SO ₄ ²⁻
Fe(II)	Function	A ₃	F ₁	D ₁	A ₃
	E _a /kJ mol ⁻¹	164±13	239±20	335±35	368±32
	ΔH [*] /kJ mol ⁻¹	157±13	231±20	325±35	361±32
	ΔS [*] /J K ⁻¹ mol ⁻¹	98±30	284±46	266±69	515±89
Ni(II)	Function	A ₃	A ₃	D ₃	A ₃
	E _a /kJ mol ⁻¹	98±24	183±20	206±9	227±28
	ΔH [*] /kJ mol ⁻¹	90±24	177±20	197±9	219±28
	ΔS [*] /J K ⁻¹ mol ⁻¹	-70±52	72±39	101±12	279±33
Co(II)	Function	A ₃	A ₃	A ₃	A ₃
	E _a /kJ mol ⁻¹	123±1	119±20	133±4	102±7
	ΔH [*] /kJ mol ⁻¹	113±1	111±20	126±4	94±7
	ΔS [*] /J K ⁻¹ mol ⁻¹	5±32	-34±45	-15±7	-57±8

Kinetic Parameters of Racemization in the Solid State		
	[Ni(phen) ₃]I ₂ ^{b)}	[Ni(phen) ₃](ClO ₄) ₂ ^{c)}
ΔH [*] /kJ mol ⁻¹	203±4	268±36
ΔS [*] /J K ⁻¹ mol ⁻¹	99±8	240±20

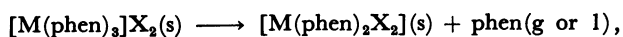
a) Notation of Sharp and co-workers (Ref. 10) is used. b) Ref. 3. c) Ref. 18.

expected to be obtained using the best function. The activation parameters obtained by the linear heating method and the isothermal method are in good agreement with each other, and the activation energy and enthalpy, E_a and ΔH^* , by the Reich-Stivala method are in good agreement with those by the Arrhenius method under linear heating conditions (Table 4). The kinetic parameters obtained are given in Table 5 with the functions which gave the best fits for the sulfates and halides of the complexes. The enthalpy and entropy of activation were calculated by the relationship: $E_a = \Delta H^* + 2RT$, $\Delta S^* = R(\ln A - \ln(kT/h) - 2)$ where the parameter, E_a and $\ln A$, were obtained by the Arrhenius equation and other parameters have their usual meanings.

The ΔH^* values for the same counterion increase with the metal in the order Co(II) < Ni(II) < Fe(II) for the bromides, iodides, and sulfates and for the chlorides, in the order Co(II) ≈ Ni(II) < Fe(II). For the same metal, the ΔH^* values increase with the counterion in the order Cl⁻ < Br⁻ < I⁻ < SO₄²⁻ for the nickel and iron complexes while the values for the cobalt complexes are almost identical for this series of counterions.

Discussion

The ligand substitution reaction of [M(II)(phen)₃]X₂ in the solid state have been reported.⁴⁾ The scheme of the reaction is as follows.



where M is Fe or Ni, X⁻ is I⁻, Br⁻, or Cl⁻, and s, l, and g

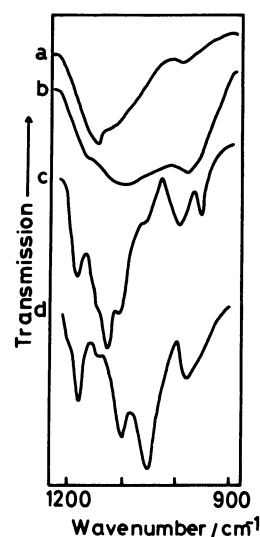


Fig. 4. Infrared spectra of sulfate ion for the complex salt, [Fe(phen)₃]SO₄. a: before heating; b: after dehydration; c: after exothermic reaction; d: product.

indicate the solid, liquid, and gaseous states, respectively. A similar reaction occurs in the case of the sulfates of all the metal complexes studied and all the cobalt complex halides studied. The coordination of the SO₄²⁻ ion to the central metal ion was confirmed by IR measurements after heating under dynamic or constant temperature conditions. If the SO₄²⁻ ion is coordinated to a metal ion, the symmetry is lowered and splitting of degenerated vibrations occurs, together with the appearance of new bands in the IR spectrum, which correspond to Raman active

bands in the free ion.¹¹⁾ These changes in SO stretching bands are observed when the sulfates are heated to the temperature where the exothermic DSC peak described above appears (Fig. 4).

It is interesting to note that the function based on nucleation and three- or one-dimensional growth, A_3 or F_1 , respectively, gives best fits for the ligand substitution of most of the complex salts while for that of the nickel(II) or iron(II) complex iodides the D_2 or D_1 function based on two- or one-dimensional diffusion, respectively, is the best fitting function (Table 5). Many mathematical models have been advanced relating nucleation and nuclei growth rates to the kinetics of phase transformation and decomposition.¹²⁾ The solid-state reaction models have been based on the assumption that the nucleation of products at active sites and subsequent growth of the nuclei occurs. In the case where all the nuclei are initially present and the growth rate of the product phase is phase-boundary controlled, the three- and one-dimensional nuclei growth equations take the forms of A_3 and F_1 , respectively. According to Laidler,¹³⁾ when a discontinuous product phase occurs, the rate-determining step may be the chemical process occurring at the phase boundary: The rate is controlled by the chemical reaction itself—that is, the breaking and re-forming of bonds at the interface. On the other hand, when material transport is the rate-controlling process (or the chemical reaction at the phase boundary is considerably faster than the transport process and thus the solid-state reaction is diffusion controlled), the functions, D_2 and D_1 , ought to be applicable in two and one dimension(s), respectively.

The defect-diffusion mechanism proposed for solid-state reactions of coordination compounds by House¹⁴⁾ may be applicable to this diffusion process. If the reaction begins with the loss of a ligand from a complex ion in a lattice site, the ligand must be placed in an interstitial position in the lattice with the formation of a Frenkel type defect. Interstitial diffusion of Frenkel defects through the lattice is enhanced by a greater difference in size between cation and anion because the volume of free space is greater when the cations and anions are of greatly differing sizes. Thus, if the dissociation occurs, the diffusion of interstitial phenanthroline would be more difficult for the iodide owing to the smaller free volume: The expected difficulty should decrease in the order $SO_4^{2-} > I^- > Br^- > Cl^-$. On the other hand, Table 5 shows the same order of anion effects on activation energies for the phase-boundary controlled nuclei growth (A_3 and F_1 : the chemical reaction itself), where the anion effects are attributed to the donicity of the lattice anions as discussed below. In the case of the iodides alone, the activation energy for the diffusion may be slightly larger than that for the chemical reaction and thus this leads to the ligand substitution

through a diffusion controlling process for the iodides.

A dissociative mechanism has been proposed for ligand substitution of several transition metal complexes in solution.¹⁵⁾ If the dissociative mechanism is also operative in the solid state, the activation parameters, ΔH^\ddagger and ΔS^\ddagger , of ligand substitution should be independent of the donicity of lattice anions. This is demonstrated by the data on ΔH^\ddagger and ΔS^\ddagger for the cobalt complex salts (Table 5).

For the nickel and iron complexes, on the other hand, changes in the lattice anion were found to alter the activation parameters, indicating an interaction of the complex cations with the anions in the transition state. Moreover, the ΔH^\ddagger and ΔS^\ddagger values of ligand substitution for the iodide of the nickel complex, $197 \pm 9 \text{ kJ mol}^{-1}$ and $101 \pm 12 \text{ J K}^{-1} \text{ mol}^{-1}$, are almost equal to those of the solid-state racemization,⁹⁾ $203 \pm 4 \text{ kJ mol}^{-1}$ and $99 \pm 8 \text{ J K}^{-1} \text{ mol}^{-1}$, respectively (Table 5). This implies that the mechanism of ligand substitution should be the same as proposed in our previous paper for the solid-state racemization of the nickel complex.⁹⁾ The mechanism involves expansion of M–N bonds to a 7-coordinate transition state with one lattice anion. If so, the rate should be controlled by the donicity of the lattice anion in the same manner as the racemization rate. Table 5 shows that the ΔH^\ddagger values for the nickel and iron complexes decrease with the anion in the order $I^- > Br^- > Cl^-$. This sequence is the same as observed for the solid-state racemization of $[Ni(bpy)_3]X_2$ ⁹⁾ and $[Co(phen)_3]X_3$,¹⁶⁾ and lies in the order of increasing donicity of the anions.¹⁷⁾ Thus, the trend in ΔH^\ddagger is attributable to the ability of the anions to stabilize the transition state by donation. In such a mechanism, a metal-anion distance will shorten with lengthening of a M–N bond(s). The interaction of the anion with the metal leads to the stabilization of the transition state and thus to a lower energy of the activation for the ligand substitution. For the iron complex, we can note that the mechanism of ligand substitution discussed above is different from that of the solid-state racemization,⁹⁾ ΔH^\ddagger values for the racemization of all the iron complex halides are identical within experimental errors ($174\text{--}178 \text{ kJ mol}^{-1}$), which can be explained by a twist mechanism.

Table 5 shows another interesting fact that the ΔH^\ddagger values for the sulfates of the nickel and iron complexes are larger than those for the corresponding iodides, respectively, despite the greater negative charge of the lattice anion, SO_4^{2-} , compared with the I^- ion. This indicates that the donicity of the SO_4^{2-} ion is lower than that of the I^- ion. Moreover, the ΔH^\ddagger and ΔS^\ddagger values of ligand substitution for the sulfate of the nickel complex, which are $219 \pm 28 \text{ kJ mol}^{-1}$ and $279 \pm 33 \text{ J K}^{-1} \text{ mol}^{-1}$ ($\Delta H^\ddagger = 254 \text{ kJ mol}^{-1}$ by Arrhenius method in Table 4), are comparable to those of the solid-state racemization for the corresponding per-

chlorate,¹⁸⁾ $268 \pm 36 \text{ kJ mol}^{-1}$ and $240 \pm 20 \text{ J K}^{-1} \text{ mol}^{-1}$, respectively (Table 5). It is reasonable to infer that the perchlorate racemizes in the solid state by a mechanism involving expansion of M–N bonds without donation of the ClO_4^- ion since the ion has negligible donor ability. The transition state for the phen substitution of the sulfate is assumed to be similar to that for the solid-state racemization of the perchlorate; thus a dissociative mechanism involving such an expansion of M–N bonds leading to bond breaking is most likely. Support for this is furnished by the relationship between E_a for ligand substitution in the solid state and the third stability constant, $\log K_3$, for the following formation reaction in aqueous media:¹⁹⁾



$\log K_3$ can be taken as a measure of the strength of M–N bonds in the tris(1,10-phenanthroline)complexes.²⁰⁾ If the rate determining step of the ligand substitution in the solid state is dominated by the ability to release a phen ligand, a linear relationship with a positive slope between E_a and $\log K_3$ for these complexes would be expected. In fact, good linearity was obtained for the sulfates (Fig. 5). Furthermore, the $\log K_3$ data show that the cobalt complex is less stable than the nickel and iron complexes and thus strength of the M–N bonds should be lower. This seems to be the reason for the change from an associative to a dissociative mechanism for the phen substitution of the cobalt complex salts.

The resultant exothermic heat of reaction for the ligand substitution of the complex salts in the solid state can be divided into two components. One is the release of one phen ligand molecule from the complex which is endothermic, and the other is the coordination of anions to the central metal which is

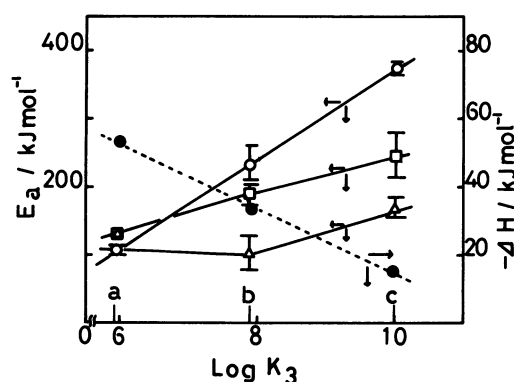


Fig. 5. Plots of activation energy (E_a : \circ , sulfate; Δ , chloride; \square , bromide) and heat of reaction of ligand substitution ($-\Delta H$: \bullet , sulfate) vs. log of consecutive stability constant ($\log K_3$) for the tris(1,10-phenanthroline)metal(II) complexes [a, cobalt(II); b, nickel(II); c, iron(II)].

exothermic. The heats of the exothermic reaction for the ligand substitution of the sulfates in the solid state also show a linear relationship with $\log K_3$ (Fig. 5); the reaction heat decreases with increasing $\log K_3$ (Table 5). This result implies that the release of phen is an important factor in lowering the reaction heat and the heat due to coordination of the SO_4^{2-} ion to all the metals is nearly identical, where there should be only an electrostatic effect. These results are consistent with the operation of a dissociative mechanism for the ligand substitution of the sulfates, suggesting negligible ability of the SO_4^{2-} ion to stabilize the transition state by donation.

In addition, the plots of E_a against $\log K_3$ for the halides for the nickel and iron complexes show that the slopes for the chlorides and bromides are nearly half the slopes for the sulfates (Fig. 5). This result may suggest that expansion of two M–N bonds to the transition state is likely for the sulfates while for the bromides and chlorides, only one M–N bond expansion occurs, although the large, rigid, flat phenanthroline ligands seem to impose considerable steric constraints on one-ended phen dissociation.⁹⁾

The heats of the exothermic reaction for the halides are smaller than those for the sulfate. This may be attributed to more difficulty of the migration of anions to the complex in the case of the halides compared to the sulfates since the process of substitution of one phenanthroline ligand in the solid state for the halides would require that two anions leave their lattice sites and enter the coordination sphere of the metal ion while for the sulfate only one lattice site is vacated. Although there is a good relationship between the activation energies for ligand substitution of the halides and the third stability constant, $\log K_3$, no correlation of the reaction heats with $\log K_3$ is observed for the halides. Factors such as covalency of M–X bonds in the products, crystal structures of the products, etc., other than strength of M–N bonds in the reactants, may be responsible for the differences in ΔH . Further research on other complexes and studies of crystal structures are required in order to understand this phenomenon. In addition, main differences in ΔS^\ddagger for the cobalt complex salts (Table 5) seem to arise from differences in the volume of free space in the lattice but at this time we have no clear explanation of the results and it is hoped that the studies of crystal structures will clarify the situation.

The present work was partially supported by a Grant-in-Aid for Scientific Research No. 57740317 from the Ministry of Education, Science and Culture.

References

- 1) See, for example, F. Basolo and R. G. Pearson, "Mechanisms of Inorganic Reactions," 2nd ed, John Wiley

& Sons, New York (1967).

2) M. Yamamoto, T. Fujiwara, and Y. Yamamoto, *Inorg. Nucl. Chem. Lett.*, **5**, 37 (1979).

3) T. Fujiwara and Y. Yamamoto, *Inorg. Chem.*, **19**, 1903 (1980).

4) K. Akabori, H. Matsuo, and Y. Yamamoto, *J. Inorg. Nucl. Chem.*, **35**, 2679 (1973); Y. Yamamoto, K. Akabori, and T. Seno, *Inorg. Nucl. Chem. Lett.*, **9**, 195 (1973).

5) L. Reich and S. S. Stivala, *Thermochim. Acta*, **34**, 287 (1979).

6) G. Beech, C. T. Mortimer, and E. G. Tyler, *J. Chem. Soc. A*, **1967**, 925.

7) E. S. Freeman and B. Carrol, *J. Phys. Chem.*, **62**, 394 (1958).

8) A. W. Coats and J. P. Redfern, *Nature*, **201**, 68 (1964).

9) M. Avrami, *J. Chem. Phys.*, **9**, 177 (1941); B. V. Erofejev, *C. R. (Dolk.) Acad. Sci. U.R.S.S.*, **52**, 511 (1946).

10) J. H. Sharp, G. W. Brindley, and B. N. N. Achar, *J. Am. Ceram. Soc.*, **49**, 379 (1966).

11) K. Nakamoto, "Infrared Spectra of Inorganic and Coordination Compounds," 2nd ed, John Wiley & Sons, New York (1970), pp. 173—175.

12) S. F. Hulbert, *J. British Ceram. Soc.*, **6**, 11 (1969).

13) K. J. Laidler, "Chemical Kinetics," McGraw-Hill, Inc., New York (1965), pp. 316—318.

14) J. E. House, Jr., *Thermochim. Acta*, **38**, 59 (1980).

15) See, for example, J. Burgess, "Metal Ions in Solution," Ellis Horwood Limited, Chichester (1978), pp. 349—404, the references cited therein, and also in Ref. 1.

16) T. Fujiwara, *Bull. Chem. Soc. Jpn.*, **56**, 122 (1983).

17) V. Gutmann and R. Schmid, *Coord. Chem. Rev.*, **12**, 263 (1974).

18) A. Tatehata, T. Kumamaru, and Y. Yamamoto, *J. Inorg. Nucl. Chem.*, **33**, 3427 (1971).

19) W. A. E. McBryde, "Critical Evaluation of Equilibrium Constants in Solution: Part A," Pergamon Press, Oxford (1978), No. 17; H. M. Irving and D. H. Mellor, *J. Chem. Soc.*, **1962**, 5222.

20) The effect of hydration on the formation reaction is almost equal for the Co(II), Fe(II), and Ni(II) complexes since the complex ions have the same charge and the same ligand. In addition, the coordination ability of water molecules is much weaker than that of 1,10-phenanthroline.
